Mining Science and Technology, 3 (1985) 51–61
Elsevier Science Publishers B.V., Amsterdam – Printed in The Netherlands

PHYSICAL MODEL STUDY OF A LONGWALL MINE

Duk-Won Park and Dwayne C. Kicker

Department of Mineral Engineering, University of Alabama, University, Tuscaloosa, AL 35486 (U.S.A.)

(Received February 1985; accepted March 1985)

ABSTRACT

In this study a new physical model for longwall mining is developed combining features of the 'sandbox' model with a new concept for excavation of mine openings using a special tool. The model is used to examine stress distributions around a longwall face in chain pillars as well as in the panel. Reproducible results are obtained, which enable a successful simulation by the model of the mode of stress changes in chain pillars, and measurement of the development of panel front abutment.

1. INTRODUCTION

An integral facet of ground control in longwall coal mining is understanding the stress distribution in the longwall panel and surrounding chain pillars as the longwall face advances. There are many available methods of study such as field measurement, analytical solution, numerical simulation and physical modeling. Usually these methods are combined for solving actual problems.

However, for complex conditions, extensive field instrumentation requires a great expense, and both numerical modeling and the analytical solution become extremely complicated. Provided that essential variables are known and proper methods are used, physical modeling can solve many problems quickly at considerably less cost.

Admittedly, rock mechanics modeling is not an easy task. It is often necessary to lessen the strength of a model material and change its physical properties in order to meet the law of similitudes. A synthetic material which will satisfy all requirements can probably never be created, therefore a compromise is necessary for practical purposes [1]. For example, if shear strength is the dominant mode of failure in the prototype, then that relationship in the model should be satisfied with all other failure modes disregarded.

The major topics in this study include development of a new model and model material, stress measuring technique and results of tests.

2. LONGWALL MINE MODEL

Harris [2] simulated the European longwall mining method using a sandbox model and examined the stress distribution around a longwall face. In the sandbox, floor strips

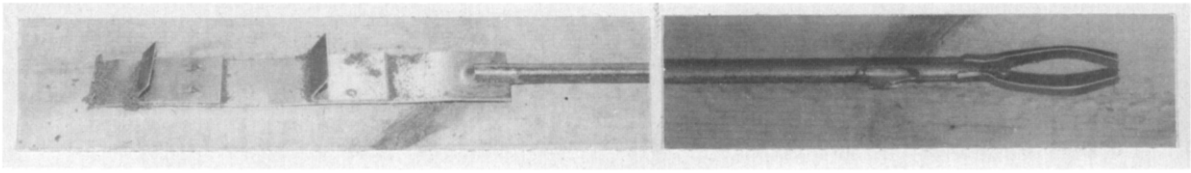

Fig. 1. Excavation tool.

were installed and they were lowered one by one, simulating gob development as a result of longwall face advancing. Miniature load cells were emplaced on the bottom of the box to monitor stress distribution in the panel and rib around the longwall panel. It has to be noted that chain pillars are not generally used in European coal mines.

In the earlier stages of the model development a similar concept was used as Harris's model. The model utilized steel rods that would slide or drop out of the bottom of the sandbox creating openings in the sand to simulate the room-and-pillar mining method [3]. However, because of the differences in compliance values between model material and steel, an uneven initial stress distribution was created during the compaction. Therefore, a new concept was developed in which the mine openings are actually excavated in the sand with a special excavation tool. The tool is a steel rod with two types of excavation devices on either end of the rod (Fig. 1). The right end allows excavation without compacting the sand, and the left end consists of a 2.54 cm (1 in.) wide scraper, which provides a clean, rectangular entry. This tool worked very effectively throughout the experiments using the improved models for chain pillar stress measurement and longwall panel front abutment.

2.1. Model material

For the physical longwall mine model, model material is required to simulate coal, which does not react to stress as a perfect elastic material but behaves as an elasto-plastic material. During the period of yielding, stress transfers from one pillar to others and some of the amount of strength is retained after failure. After various model materials were tested, a sand and oil mixture was found well suited for simulating the behavior of coal.

Locally available quartz sand was used. The size distribution of the sand is shown in Table 1. Six different combinations of sand and oil mixtures were made using two types of heavy oil, 250 SAE and 90 SAE. The ratios of oil and sand and density are shown in Table 2. It was noticed that the density was influenced by the ratio of oil and sand. For both types of oil, the maximum density was attained when the ratio was 73.9 cc (2.5 oz.) of oil per 0.45 kg (1 lb.) of sand (mixtures Nos. 2 and 6).

A direct shear strength test was performed on each mixture with various normal loadings, using a regular direct shear-testing machine for soil. The typical relationships between horizontal displacement and horizontal load for a constant normal load is shown in Fig. 2. The slope is steep during the first stage

TABLE 1

Particle size distribution of sand used as model material

Size		Weight (g)	Percentage
Mesh	mm		
>16	+1.4095	4	0.99
16–48	−1.4095+0.295	76	18.72
48–70	−1.2950+0.199	196	48.28
70–80	−1.1990+0.182	50	12.30
80–100	−0.1820+0.147	55	13.55
<200	−0.1470+0.074	25	6.16

TABLE 2

Composition of model material and density

Mixture no.	250 SAE oil, cc (*oz.*)	90 SAE oil, cc (*oz.*)	Sand kg (*lb*)	Density, g/cc
1	44.4 (*1.5*)		0.45 (*1*)	1.70
2	73.9 (*2.5*)		0.45 (*1*)	1.82
3	94.5 (*3.2*)		0.45 (*1*)	1.66
4		44.4 (*1.5*)	0.45 (*1*)	1.50
5		29.6 (*1.0*)	0.45 (*1*)	1.63
6		73.9 (*2.5*)	0.45 (*1*)	1.78

and it becomes gentler, simulating the strain-softening phenomenon. After the maximum shear stress is reached, some strength is maintained for a period of time and gradually decreases, showing quite a long period of plastic failure. When four or five values were obtained using different normal stresses, a graph of the shear strength versus normal stress was plotted to obtain cohesion and the internal friction angle. Most of them showed a linear relationship.

Both mixtures showed low cohesion; the 250 SAE mixture had an average cohesion of 0.28 bar (4.0 psi) and the 90 SAE mixture had 0.15 bar (2.0 psi). However, internal friction angles were 33.3° for the 250 SAE mixture and 39° for the 90 SAE mixtures. Slight variations were noticed in internal friction angles for the different oil/sand ratios. In summary, higher-viscosity oil reduced the internal friction angle while increasing the cohesion.

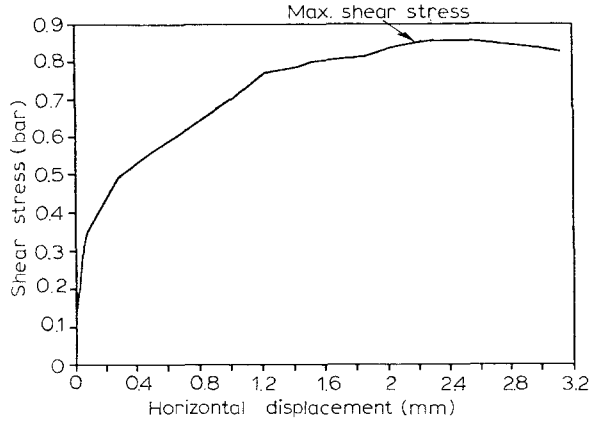

Fig. 2. Shear stress versus horizontal displacement for model material.

Throughout this study, mixture No. 1 was used as the model mateiral for the first layer.

2.2 Stress measuring techniques

For this model, it is critical to select adequate means of measuring stress distribution in the chain pillars or the longwall panel. Because of the fact that stress change in the model is quite small, the measuring device should be sensitive enough to detect extremely small stress changes, and the physical size of the device should be small enough so as not to disturb the stress distribution by emplacing them in the model pillars. Miniaturized load cells, the latest state-of-the-art technology, have provided excellent results. Each load cell incorporates semiconductor strain gages in a fully active Wheatstone bridge configuration. The load cells are powered by 15 V DC excitation and have built-in temperature compensation, as well as individual calibration. They are 2.79 mm (0.11 in.) in thickness with a 12.7 mm (0.50 in.) diameter, allowing the stress of a small point to be measured. The resolution of the load cells is 67 Pa (0.01 psi). The load cells are commercially available from Entran Devices, Inc. and further specifications are provided in Entran Bulletin ELF5005-881.

The model used a maximum of 12 load cells, all of which are monitored by two switching and balancing units connected in series. A constant 15 V is supplied by a voltage regulator connected to the power terminals of one switch and balance unit, and the output voltage across the signal terminals is recorded by a voltmeter. By recording the output voltage from the load cell circuit and applying the calibration factor, the load on each cell can be calculated.

2.3 Chain pillar stress measurement

The model consists of a box constructed of 19 mm (3/4 in.) plywood, 74.9 × 120.6 × 50.8 cm, mounted on a table. The box rests on the table at its four corner posts so that a 12.7 mm (0.5 in.) slot is left around the bottom perimeter of the box. This allows a flexible layout of entries and panels, which are accessed through these openings.

To create entries, the excavating tool is guided along its desired path by metal plates, 1.3 mm (0.05 in.) in thickness, which are secured on the table top where pillars are to be created (Fig. 3). The tool is then guided by the edge of the plates.

To effectively simulate stress distribution in the chain pillars, four entries were driven across the width of the model along its central area, so that a longwall panel is created on either side of the set of entries. Each panel actually represents only half of the total panel width, which is that portion of the panel affecting the stress in the chain pillars. Each pillar is 12.7 × 12.7 cm (5 × 5 in.), and the half width of the panel is 35.6 cm (14.0 in.) The width of the entry is 2.54 cm (1 in.) and the height is 1.27 cm (0.5 in.).

Each entry is cut from one side of the box and each crosscut is cut from the adjacent side. Therefore, the only access to the crosscuts is through the panel. To aid in the mining of the crosscuts, metal rods were placed on the table top extending from outside the box through the 12.7 m (0.5 in.) slot to the pillar edge where each crosscut is to be made (Fig. 3). Then, as the model is loaded, these rods are removed to create openings through the panel so that the excavating tool can begin cutting the crosscuts guided by the pillar plates.

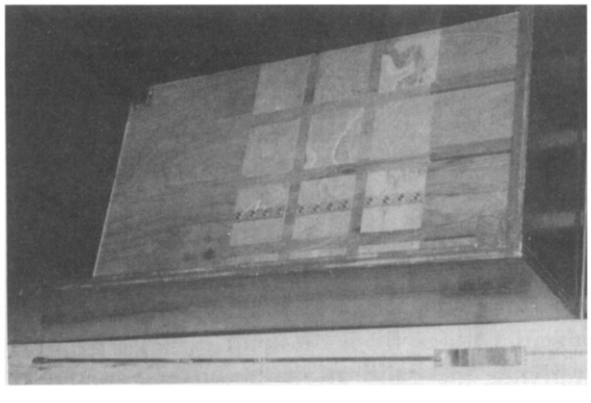

Fig. 3. Sandbox longwall mine model (top view).

The stress was chosen to be measured in three chain pillars parallel to the direction of the longwall face. Four load cells were mounted in each pillar as shown in Fig. 4(a). A thin plastic strip was first secured to the metal guide plates and the load cells were placed on the plastic strip to aid in careful removal of the load cells.

A series of three tests were completed with overburden depths of 34.3 (Test 1), 22.9 (Test 2), and 15.2 (Test 3) cm. Each test had a common 10.2 cm (4 in.) layer of wet sand (sand/oil mixture) compacted to approximately the same pressure, and a second layer of dry sand varied to meet the desired overburden thickness.

The mining procedure was kept the same for each test. The entries were completed in 24 intervals, where at each interval, each load cell reading was recorded. As the mining activity neared the load cell area, more intervals were taken. Each longwall panel was mined in 14 intervals.

2.4 Longwall panel front abutment measurement

The same model used to measure chain pillar stress was also used to measure front abutment pressure in the panel. The layout was changed to simulate a 43.2 cm (17 in.) wide panel with a 50.8 cm (20 in.) advance over a portion of the model as shown in Fig. 4(b). Notice that the line of load cells at the end of the advance covers 30.5 cm (12 in.) of the panel width. This represents half of the

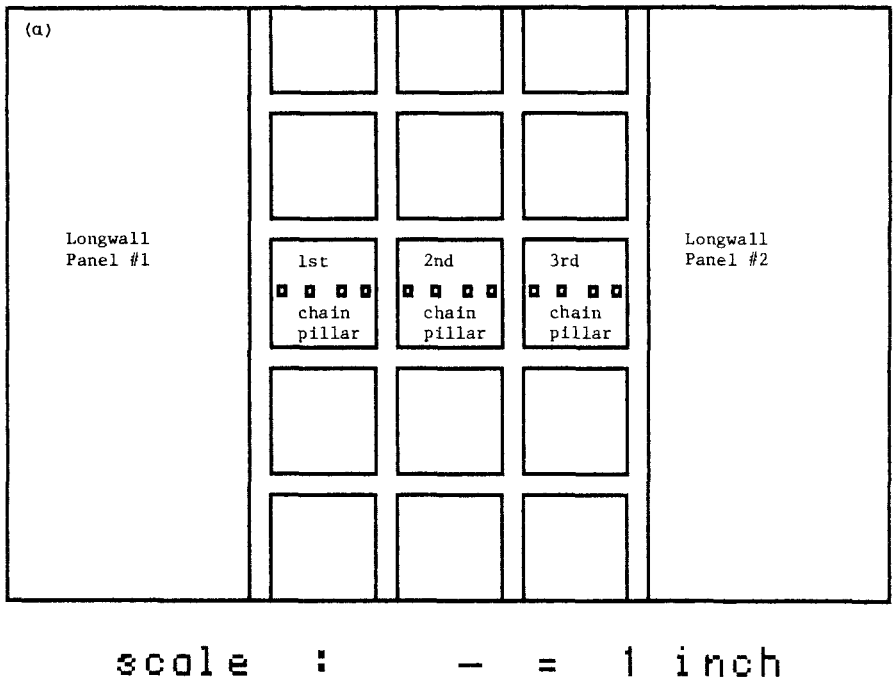

Fig. 4(a). Layout of chain pillar model.

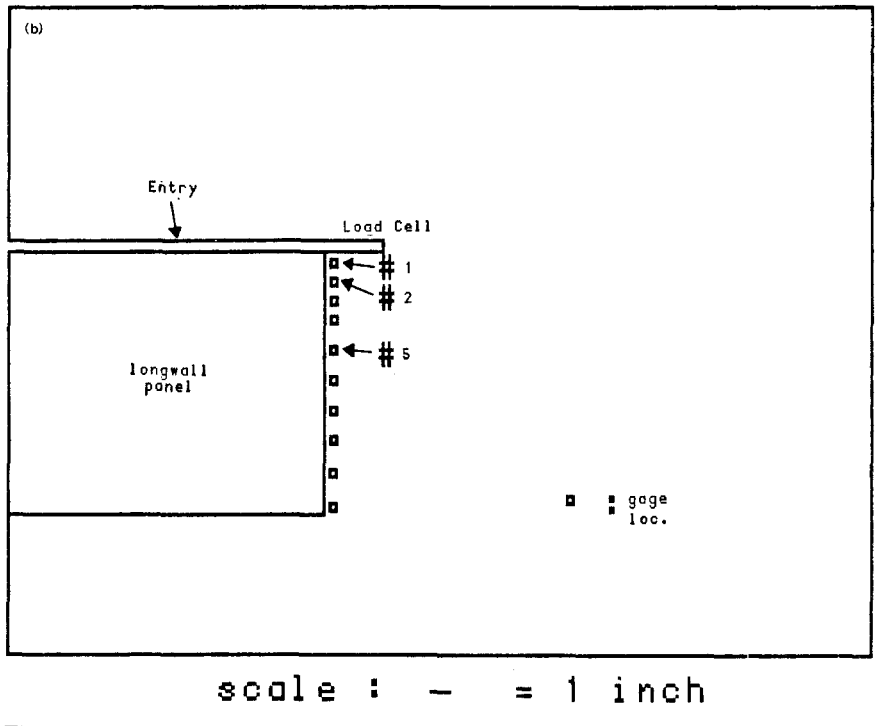

Fig. 4(b). Layout of front abutment model.

total panel width. The remaining 12.7 cm (5 in.) width is there to reduce the effects of the model wall on the panel stress distribution. The inside boundary of the panel is the model wall and the outside edge is created by a single entry.

The first step in the procedure is to mine the single entry. The first 35.6 cm (14 in.) of the entry is created by removing a steel rod. The excavating tool is then used to extend the entry another 15.2 cm (6 in.) for a total length of 50.8 cm (20 in.). The entry is excavated in this manner so that the rod does not produce any unrealistic stress distributions around the load cell area.

The next step is to mine the panel, which is advanced in approximately 2.54 cm (1 in.) intervals until the face reaches the load cell line.

3. RESULTS OF TESTS

3.1 Chain pillar

The stress distribution in the chain pillars for each test was very similar, with reproducible trends occurring at each test run. As mining approached the load cell area, stress in that area generally increased. Once the mining activity reaches the load cell location, a sharp decrease occurs at the two load cells nearest the mining activity, while other areas continued increasing. Therefore, initial failure is occurring at the pillar edges. This effect is illustrated in Fig. 5, which shows the stress distribution across the three chain pillars for different stages of mining. A negative sign indicates the face distance from the load cell area and a positive sign indicates the advance past the load cell area. This sign convention is used throughout each experiment. However, after this initial failure, the pillar edges generally begin to handle more stress as the face continues to advance. At the completion of the entries, higher stress along the pillar edge is more evident in the tests with low overburden pressures than in the tests with higher pressures. With high overburden pressures, drastic failure sometimes occurs along the pillar edge, in which low stress was continually measured throughout the period of entry development (Fig. 5). Also, at the completion of the entries, the highest stress generally occurs in the middle pillar, indicating a stress transfer to this area (Fig. 6).

As the longwall face approaches the load cell area, the stress in pillar nearest to the panel begins to increase, though some fluctuation of stress level occurs across the width of the pillar. Then, as the face reaches the load cell area, a sharp decrease in stress occurs along the pillar edge, with progressively less decrease across the pillar width. As this decrease in stress, or pillar failure occurs in the first pillar, a slight stress increase occurs in the middle pillar, indicating a stress transfer from the first pillar to the middle pillar. Little stress change is noted in the third pillar during this period (Fig. 7).

These results agree with those obtained from a numerical modeling conducted by Park and Ash [4]. In their study, strain softening behavior of rock and coal layers around a coal mine opening was simulated using a quasi-elastic approach, which accounts for residual strength after failure. This simulation was achieved in such a way that material values were modified after each run according to stress distribution until it reached an equilibrium condition. The results agreed with the field measurement conducted in an Alabama coal mine. Three typical stages of stress redistribution are shown in Fig. 8, which can be compared with Fig. 5.

The pillar nearest to the panel continues to show a stress decrease for a face advance approximately 5 cm (2 in.) past the load cell area. At this point, a stress increase occurs. Again, the stress increase is somewhat proportional across the pillar width, with the highest increase along the pillar edge nearest the panel

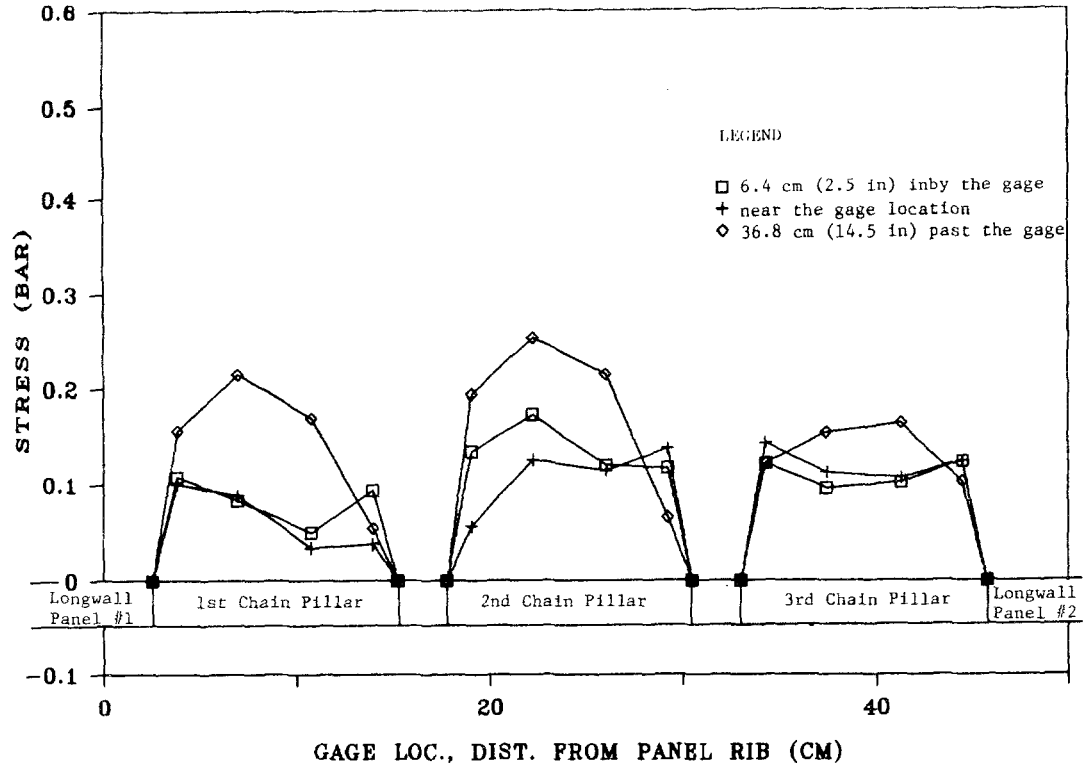

Fig. 5. Stress distribution during entry development.

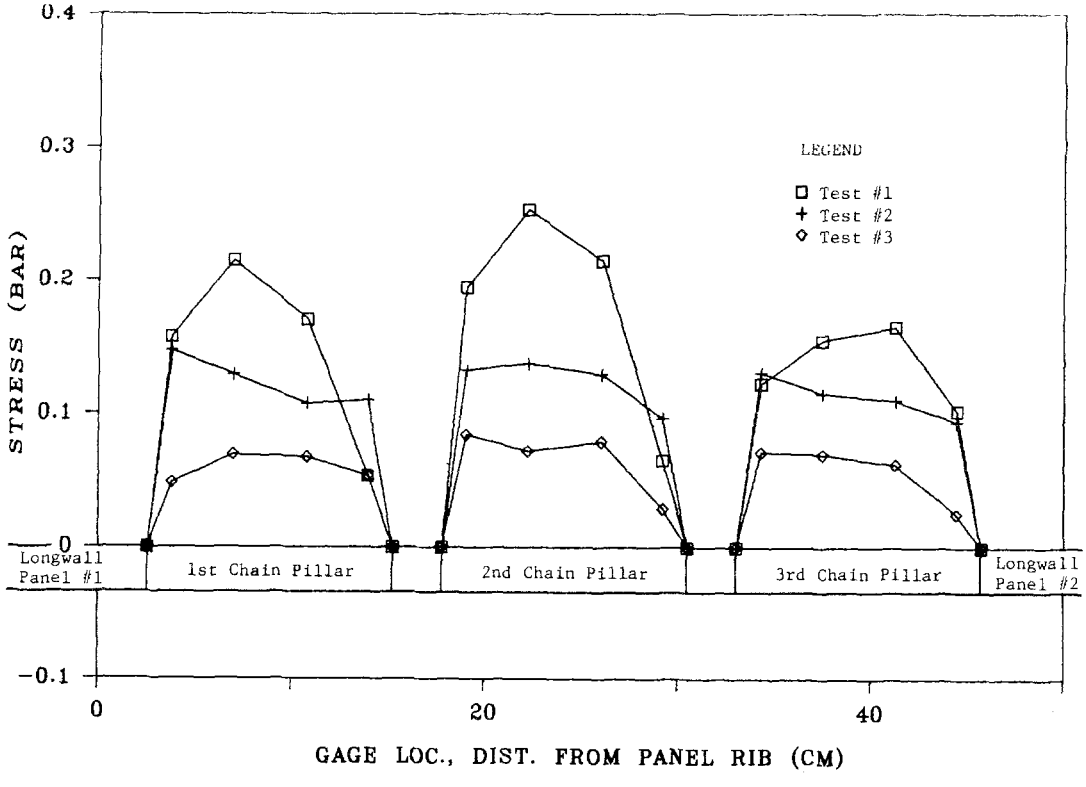

Fig. 6. Stress distribution across chain pillars at completion of entries.

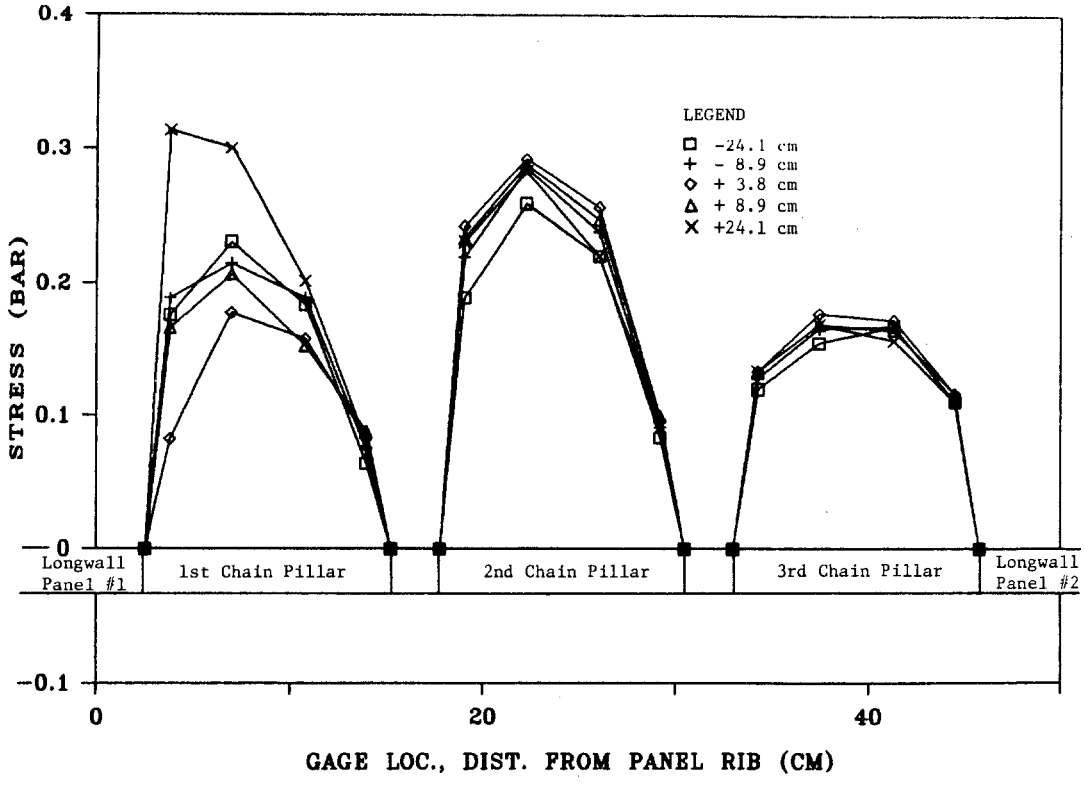

Fig. 7. Stress distribution across chain pillars during advance of long wall panel 1.

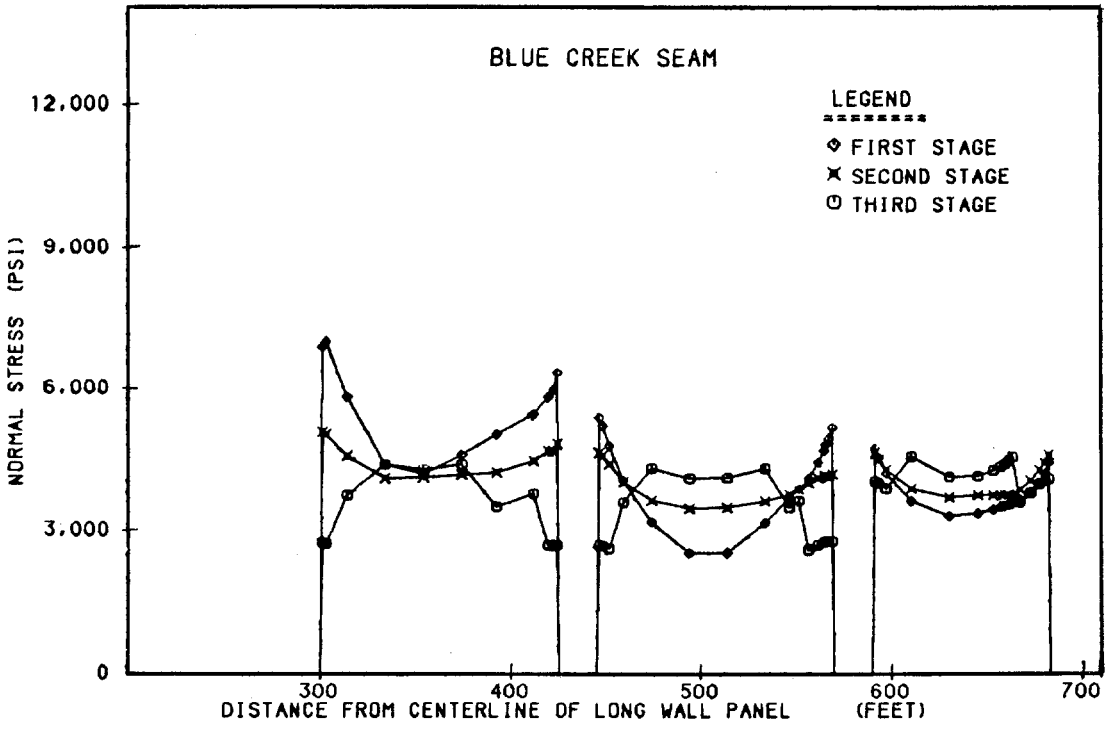

Fig. 8. Stress distribution across chain pillars obtained from finite element method (after Park and Ash, ref. 4)

and the lowest increase on the opposite pillar edge. As this happens, a slight decrease in stress occurs in the second and third pillars, indicating a stress transfer again, back to the first pillar (Fig. 7). Apparently, as the roof is allowed to cave behind the face, a recompaction of the sand occurs over the pillar near the gob area, causing the stress transfer.

Similar effects are noticed as panel 2 is mined: the same type pattern of stress increase as face approaches the load cell area, a sharp decrease in stress at the load cell area, then a sharp increase as the face continues to advance. The stress along the pillar edge farthest from the active panel still remains high, but a stress decrease is noticed (Fig. 9).

A general trend in the manner of stress transfer is noticed in the models with higher overburden pressure. As stated, the stress in the pillar near the active panel shows an overall increase. The maximum stress decrease in the other two pillars occurs along the edge farthest from the active panel. This effect is illustrated in Fig. 7 and Fig. 9.

3.2 Front abutment

As the model was loaded, the initial stress across the width of the panel varied slightly. However, the effects of mining produced similar stress changes in each load cell. During entry development, the load cells near the entry (cells 1 and 2) show a decrease just as in the chain pillar model, as shown in Fig. 10. As the panel edge begins to fail, stress inside the panel (cell 5) increases. Then, as the face begins to advance, the stress remains fairly constant, even decreasing in some cases until a significant stress increase occurs at about 20 cm (8 in.) ahead of the face. As mining con-

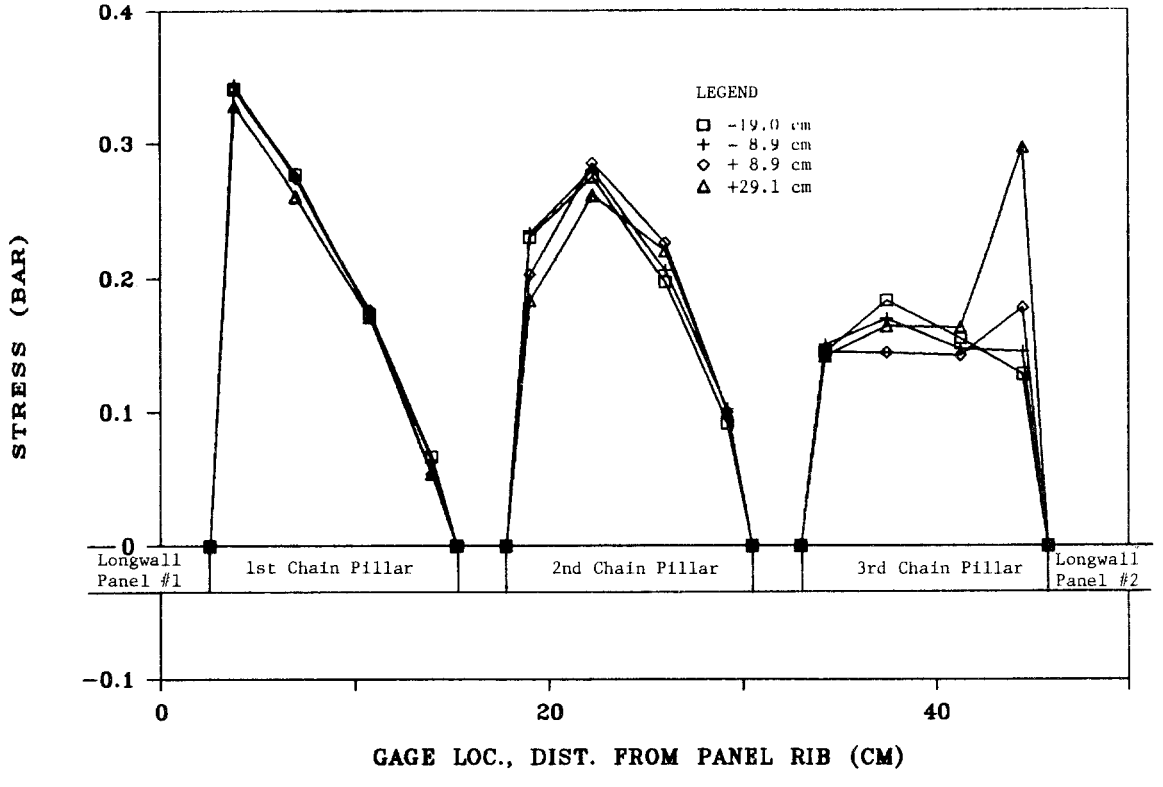

Fig. 9. Stress distribution across chain pillars during advance of longwall panel 2.

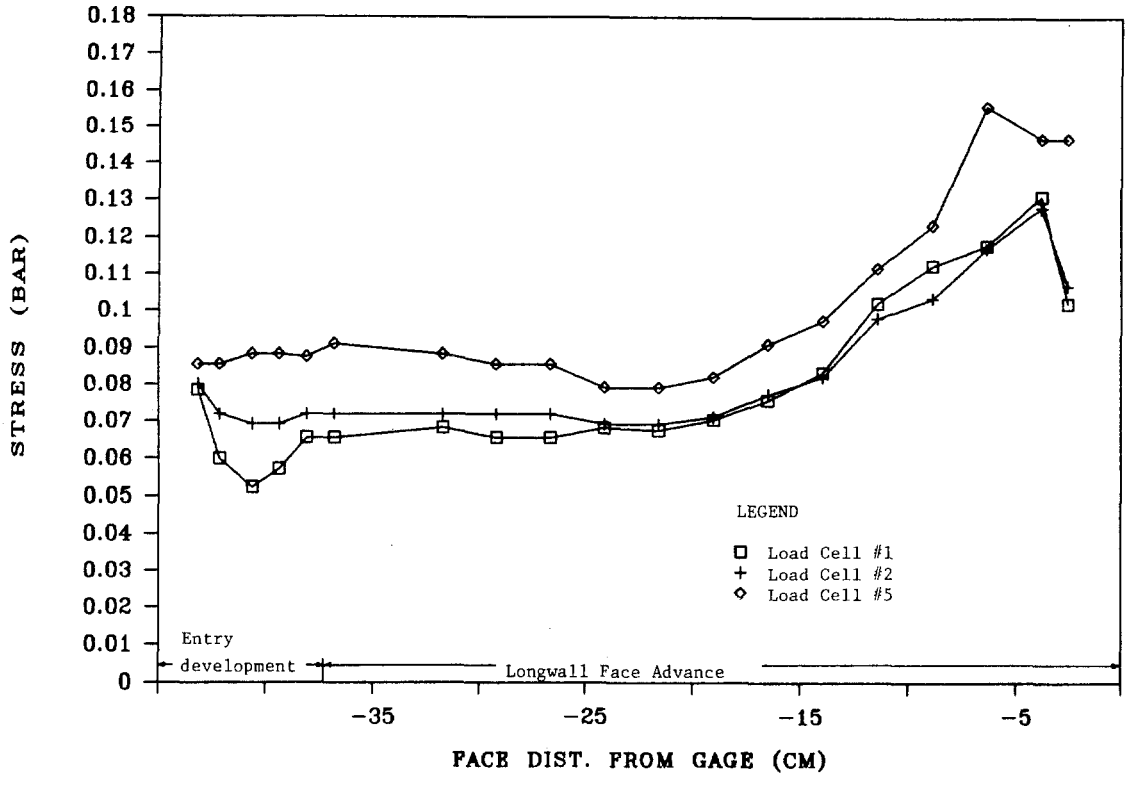

Fig. 10. Development of front abutment stress.

tinues, the stress in each load cell, though initially varied, begins to converge to the same level. The innermost load cell (5) in Fig. 10 reached the maximum stress at 6.4 cm (2.5 in.) from the face. The two load cells near the panel edge also converged to the same maximum stress at 3.8 cm (1.5 in.) from the face.

4. CONCLUSIONS

A new physical longwall mine model was developed to study stress distributions around a longwall face in both the chain pillars and panel. State-of-the-art stress detection devices combined with a new excavation technique and model material have provided reproducible results on the manner of stress re-distributions caused by longwall mining. The model has successfully simulated the mode of stress changes in the chain pillars and has measured the development of the panel front abutment.

To increase the capability of the model, the laws of similitude [5] and dimensional analysis [6] should be applied to the model to prototype relationships. Many of the pertinent variables of this model study are related to the model material. Therefore, the development and application of other model materials should enhance the model. With continued research and refinement, the model can become more beneficial in the understanding of stress distributions around a longwall panel.

ACKNOWLEDGEMENT

The work was funded by the Bureau of Mines, U.S. Department of the Interior, through Virginia Polytechnic Institute and State University, as a research project of the Generic Mineral Technology Center in Mine System Design and Ground Control.

REFERENCES

1 L. Obert and W.I. Duvall, Rock Mechanics and the Design of Structures in Rock, Wiley & Sons, New York, NY, 1967, pp. 387–401.

2 G.W. Harris, A sandbox model used to examine the stress distribution around a simulated longwall coalface, Int. J. Rock Mech. Min. Sci. Geomech., 11 (1974) 325–335.

3 D.W. Park, R.L. Sanford, T.A. Simpson and H.L. Hartman, Pillar stability and subsidence study at a deep longwall coal mine, Proc. Ann. Workshop, Generic Min. Tech. Center, Mine Systems Design and Ground Control, Virginia Polytechnic Institute and State University, Blacksburg, VA, 1983.

4 D.W. Park and N.F. Ash, Stability analysis of entries in a deep coal mine using finite element method, Mining Science and Technology, 3 (1) (1985): 11–20 (this issue).

5 G. Murphy, Similitude in Engineering, Ronald Press, New York, NY, 1950, pp. 57–66.

6 H.L. Langhaar, Dimensional Analysis and Theory of Models, Wiley & Sons, New York, NY, 1951, pp. 60–65.